JOURNAL OF GEOPHYSICAL RESEARCH, VOL. 87, NO. B8, PAGES 6771–6780, AUGUST 10, 1982

Strain Hardening and Strength of Clay-Rich Fault Gouges

C. A. MORROW

U.S. Geological Survey, Menlo Park, California 94025

L. Q. SHI

State Seismological Bureau, Beijing, People's Republic of China

J. D. BYERLEE

U.S. Geological Survey, Menlo Park, California 94025

Frictional sliding experiments at confining pressures from 50 to 400 MPa were performed on thin layers of clay-rich fault gouges from locations along the San Andreas and Hayward faults in California as well as pure clays from other locations. Both dry and saturated, drained samples exhibited a strain hardening that increased systematically with increasing confining pressure for the each particular gouge. In addition, the amount of strain hardening was greater with progressively stronger gouges among the suite of different samples. Tests using various lubricating mediums at the sample ends and different jacketing materials all showed that these possible constraints on frictional sliding had no effect on the strain-hardening process. Therefore, the observed strain hardening was a material property of the fault gouges. The presence of water lowered the strength, coefficient of friction, and amount of strain hardening of the samples. The coefficient of friction ranged from around 0.21 to 0.58 under saturated, drained conditions at 200-MPa confining pressure with the exception of pure montmorillonite. This sample had anomalously low strength and friction ($\mu \sim 0.13$) in relation to the other specimens. The strength of the gouges did not correlate well with mineral composition, grain size distribution, or location along the San Andreas fault; in particular, gouge samples from creeping and 'locked' sections of the fault showed no systematic differences in strength.

INTRODUCTION

Rock-on-rock and rock-gouge experiments have received much attention in an effort to understand the mechanism of naturally occurring fault slip [e.g., *Summers and Byerlee, 1977a, b*; *Shimamoto and Logan, 1981*; *Wang et al., 1980*]. Shearing characteristics of laboratory samples (stable sliding, stick slip) are frequently likened to the fault creep or earthquake activity observed along fault zones [*Byerlee, 1968*]. Regardless of the stability and frictional properties of the material, laboratory strength curves often show a material strengthening with displacement that depends on material composition, degree of saturation, temperature, and stress. This characteristic has been demonstrated for granular materials, soils, and clays [*Zoback and Byerlee, 1976*; *Mitchell, 1976*; *Lambe and Whitman, 1969*] as well as with frictional experiments both with and without thin gouge layers [*Summers and Byerlee, 1977a, b*; *Shimamoto and Logan, 1981*]. If frictional studies are indeed an appropriate analogue for earthquake problems, do these results imply that active crustal faults become stronger with time prior to failure?

It has been argued that the strain hardening observed during frictional sliding experiments may not be a real material property but rather may be an artifact of the measuring technique. Many standard triaxial frictional strength experiments utilize a cylindrical rock sample with a saw cut inclined to the cylindrical axis. When this assembly undergoes axial shortening, there must be a small sideways movement of the sample halves as they slide past each other, resulting in a misalignment of the sample column. If frictional tractions are created between the sample and the end plugs that resist this misalignment, then an apparent strengthening of the sliding surfaces may result. Laboratory observations are not likely to be analogous to natural fault behavior in this case.

This study examines the extent to which these mechanical constraints influence the rheological behavior of fault gouge material as well as general aspects of strain-hardening properties and strength under both dry and wet conditions. For this reason, a series of frictional sliding experiments were carried out under high pressure using clay-rich fault gouges from various locations along the San Andreas and Hayward fault traces.

GOUGE DESCRIPTION

The principal gouge used in this study was collected from a road cut at Tejon Pass in the San Gabriel Mountains. This gouge is composed mainly of montmorillonite and mixed-layer (montmorillonite/illite) clays with lesser amounts of illite and chlorite and a trace of kaolinite. The material is homogeneous and extremely fine grained, 94% of the grains being less than 0.063 mm in diameter. Other natural gouges in this study are from locations along or near the San Andreas and Hayward faults. These inlcude serpentine-rich (D Street Hayward and Golden Gate Bridge, San Francisco), chlorite-rich (Strain Ranch), and mixed assemblage samples (Cienega Valley and Dry Lake Valley). Sampling was from surface outcrops with the exception of the Cienega Valley and Dry Lake Valley gouges, which were taken from drill cores at 402 and 218 m, respectively. Three nongouge clays composed of pure kaolinite, montmorillonite, and illite were included for comparison. X ray analyses of the specimens

Paper number 2B0791.
0148-0227/82/002B-0791$05.00

TABLE 1. Mineralogical Composition of Gouges and Clays by Weight Percent

Name of Gouge or Clay	Chlorite	Kaolinite	Illite	Montmoril-lonite	Mixed Layer Mont/Illite	Serpentine
Strain Ranch San Andreas Gouge Marin County	72	15	8	...	5	...
Cienega Valley San Andreas Gouge San Benito County	6	14	8	26	46	...
Dry Lake Valley San Andreas Gouge San Benito County	11	28	12	16	33	...
Tejon Pass San Andreas Gouge Los Angeles County	10	trace	20	38	32	...
D St. Hayward Fault Gouge	...	...	...	...	...	100
Golden Gate Bridge Fault Gouge	...	...	...	...	...	100
Kaolinite Lincoln, Calif.	...	100	...	...	...	...
Montmorillonite Chambers, Ariz.	...	...	...	100	...	...
Illite Fithian, Ill.	...	...	100	...	...	...

Weight percent ±2%.

are given in Table 1. Table 2 contains a grain size distribution of the gouges obtained using both wet and dry sieving methods. Sampling locations are shown in Figure 1.

EXPERIMENTAL PROCEDURE

Cylindrical samples of Barre granite, 2.54 cm in diameter and 6.35 cm long, were cut in half along a plane oriented at an angle of 30° to the cylindrical axis (Figure 2). The granite halves were separated by a 1.0-mm-thick layer of powdered gouge along the saw cut. For the dry strength tests, the gouge was vacuum dried in an oven overnight. For the wet strength tests, the gouge was presaturated with a small amount of distilled water to allow molding of the sample onto the granite surface. A 0.13-mm-thick copper sleeve held the two pieces of granite and the gouge together. Steel spacers were then placed at either end of the sample. For some experiments, these spacers were left unlubricated. In others, a thin layer of molybdenum, lead, teflon, or talc was applied to the surface of the spacers. The entire assembly was then jacketed in polyurethane to isolate the sample from the confining pressure fluid. The confining pressure was held constant by a computer-controlled servomechanism, and the sample was vented to atmospheric pressure.

An axial load was applied to each sample at a strain rate of 10^{-6}/s, resulting in a slip rate along the gouge-filled saw cut of 7.33×10^{-5} mm/s. The samples slid for 10 mm before the experiments were terminated. All stress data were corrected for the decreasing area of contact between the two surfaces with displacement.

The first series of experiments was designed to investigate whether or not the apparent strain hardening of the fault gouge is due to experimental factors, such as the previously mentioned frictional tractions between the sample and the steel end plugs, or due to the strength of the jacket material. Both of these factors may tend to inhibit the lateral motion of the granite pieces as they slide along each other. To test the frictional traction effect, vacuum-dried samples of Tejon Pass gouge were deformed at 200 MPa and 400 MPa confin-

TABLE 2. Grain Size Distribution of Gouges and Clays

Name of Gouge or Clay	Grain Size Distribution, wt %								
	>2 mm	1–2 mm	0.5–1 mm	0.25–0.5 mm	0.125–0.25 mm	0.09–0.125 mm	0.063–0.09 mm	0.045–0.063 mm	<0.045 mm
Strain Ranch, San Andreas	15.2	4.3	3.7	3.8	5.9	2.5	3.4	2.2	59.0
Cienega Valley, San Andreas	0.2	...	...	0.1	0.4	0.3	0.7	0.5	97.8
Dry Lake Valley, San Andreas	...	0.1	...	...	0.4	0.8	3.3	3.3	92.1
Tejon Pass, San Andreas	0.1	0.3	0.3	0.8	2.2	1.3	1.5	2.2	91.3
D St. Hayward Hayward Fault	5.1	2.1	2.6	6.3	25.2	17.5	16.8	-----24.2------	
Golden Gate Bridge	0.5	1.3	3.4	13.1	37.8	18.5	----------25.4----------		
Kaolinite	...	...	...	...	...	...	0.2	0.2	99.6
Montmorillonite	...	...	...	...	1.0	4.4	1.9	2.8	89.9
Illite	...	...	...	...	1.3	3.0	1.4	6.1	88.2

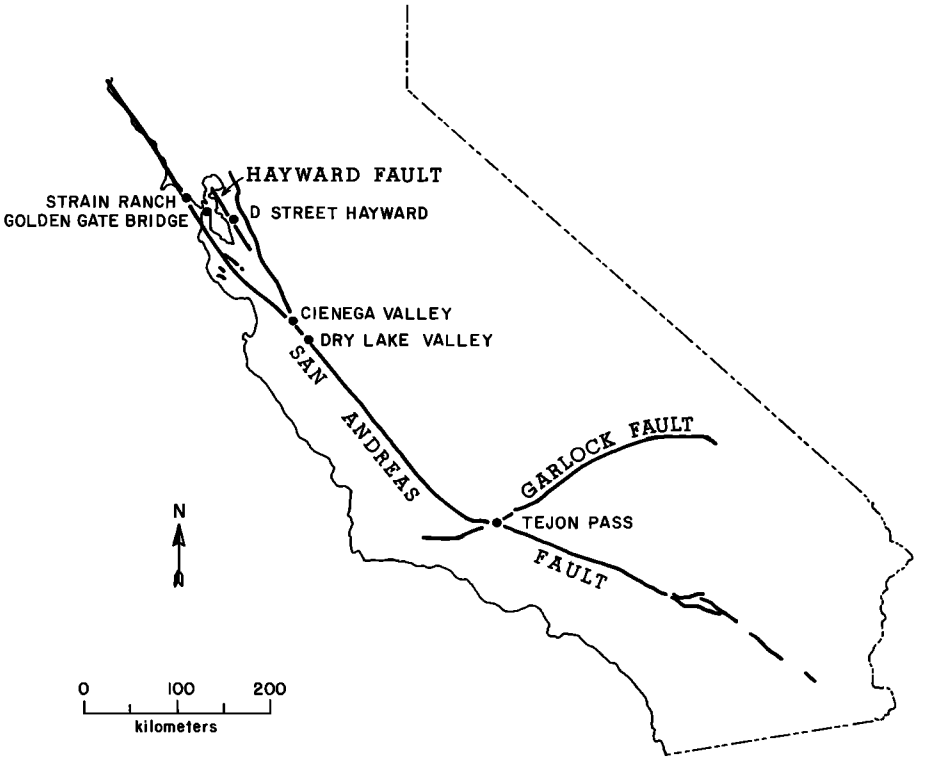

Fig. 1. Gouge sample locations in California.

ing pressure by using a number of different lubricating mediums at the steel spacers and also using no lubrication. A stiff jacket material might also cause an apparent strenghening or strain hardening of the gouge because the jacket will resist the bulging required to accommodate the sliding sample. As a number of different materials are frequently used, their behavior should be understood. This stiffness effect was tested by using both rubber (complaint) and polyurethane (stiffer) jackets around the samples.

After these experiments concerned with mechanical constraints on the system, the material properties of the Tejon Pass gouge were investigated as a function of stress. Of interest were the strength, coefficient of friction, strain hardening, creep, and stick slip behavior. The gouge was deformed at confining pressures from 50 to 400 MPa after being vacuum dried and also under wet, drained conditions, as described by *Morrow et al.* [1981]. End lubricant was not applied for these experiments. Last, strength and strain-hardening effects were observed for specimens of differing compositions. For these experiments, saturated samples of the pure clays and clay-rich San Andreas gouges described in Table 1 were deformed at 200-MPa confining pressure.

RESULTS

The strengths of dry Tejon Pass gouge deformed at 200 and 400 MPa confining pressure using different types of sample end lubrication are shown in Figure 3. All samples exhibited strain hardening after the initial elastic portion of the stress-strain curve. Both the strength and the amount of strain hardening were higher at 400 MPa. There is little difference between the unlubricated and lubricated specimens other than that expected from variations among samples. Strength was not consistently higher for one type of lubrication than for another at the two confining pressures nor was there any sytematic order to the onset of stick slip behavior. The slopes of the curves at each pressure were nearly the same. Most importantly, the unlubricated sample was not in any way distinct from the others. Therefore, frictional resistance at the ends of the sample did not influence the strain hardening or strength of the system, and the unlubricated case was a representative experiment.

Jacket stiffness appeared to have an effect on the strength of the Tejon Pass gouge (Figure 4). The sample sealed in a

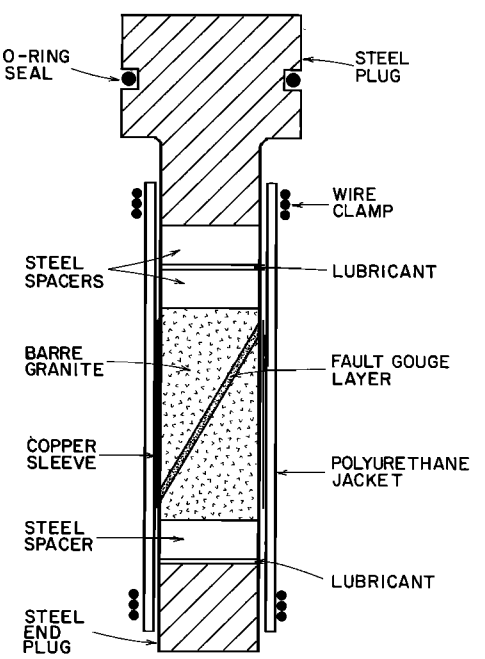

Fig. 2. Experimental assembly.

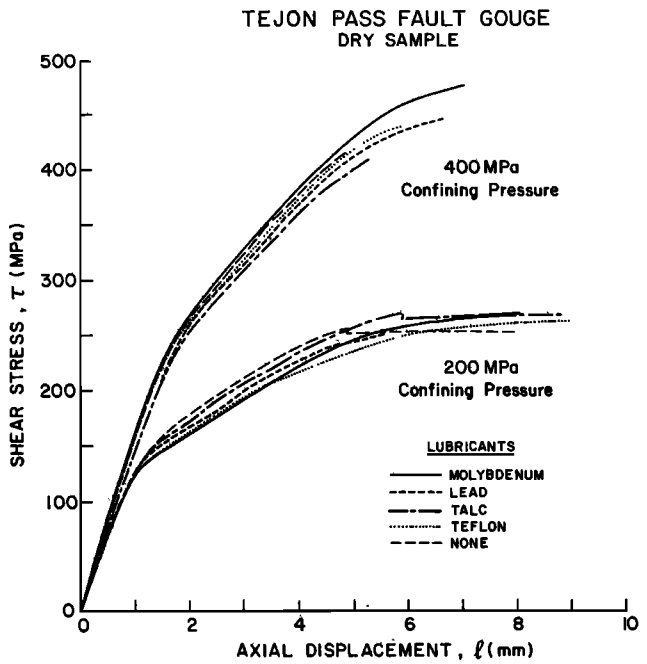

Fig. 3. Strength of dry Tejon Pass fault gouge under confining pressures of 200 and 400 MPa with and without sample end lubrication.

polyurethane sheath was about 20 MPa stronger than the rubber-jacketed sample under the same experimental conditions, as we might expect from a stiffer material. The more compliant rubber probably does not offer much resistance to shearing, as the rubber is more easily able to accommodate the changing configuration of the sample. Rubber was not used in further experiments because of its chemical reaction with the confining fluid. From Figure 4, we estimate an uncertainty in the absolute strength of about 10%. The interesting point to note, however, is that the slopes of the loading curves were quite similar for these two experiments. The same amount of hardening occurred in both the rubber-jacketed samples and with the stiffer polyurethane jackets. This observed strain hardening must be, therefore, a material property of the gouge that is affected neither by the strength of the jacket nor by the frictional resistance to lateral displacement at the sample ends. Accordingly, further experiments were carried out with the more reliable polyurethane jackets, and no lubrication was used between the steel spacers and the end plugs.

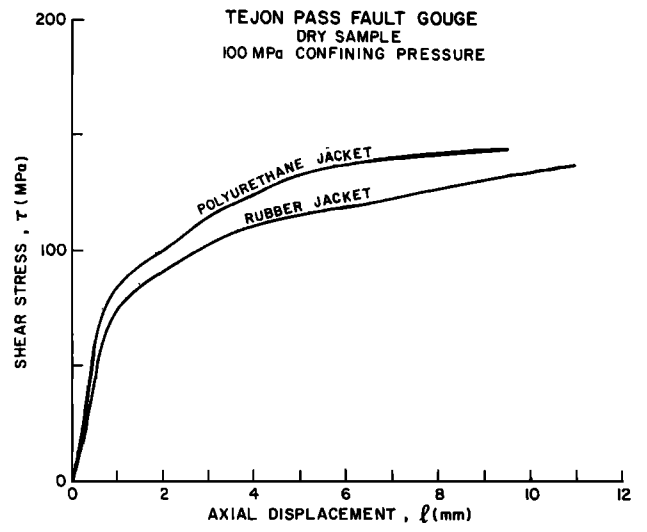

Fig. 4. Effect of jacket material (rubber and polyurethane) on the strength of Tejon Pass gouge under 100-MPa confining pressure.

The strength of dry Tejon Pass gouge under confining pressures from 50 to 400 MPa is shown in Figure 5. Strength characteristically increased with higher confining pressure. There are three typical stages to the stress-strain curves: an initial elastic stage, with a high shear modulus; followed by a period of strain hardening with a lower but relatively constant modulus; and finally, a decrease of this modulus into a period of stable sliding, during which stresses did not rise appreciably with displacement. Sliding progressed smoothly and was not characterized by numerous small stress drops as was observed with saw cut surfaces of granite [*Summers and Byerlee*, 1977*b*; *Scholz et al.*, 1972]. Stable sliding was terminated by one sudden, large stress drop in all cases except at 50 MPa (Figure 5). In general, sample failure occurred after smaller amounts of displacement following each increase in confining pressure, resulting in progressively shorter creeping periods. At the highest pressures (300 and 400 MPa), stick slip occurred as the modulus was decreasing, before the onset of creep. These characteristics give the strength curves of Figure 5 the appearance of elastic-plastic behavior at low pressure, changing to brittle behavior at high pressure, consistent with the brittle-ductile transitional behavior for sliding surfaces described elsewhere [*Byerlee*, 1968; *Logan*, 1977; *Stesky*, 1978].

Peak shear stress plotted as a fucntion of normal stress (Figure 6) at the different confining pressures delineates a failure envelope that can be expressed approximately as

$$\tau = 12.2 \text{ MPa} + 0.73\sigma_n$$

where σ_n is the normal stress across the sliding surfaces and τ corresponds to the maximum shear stress achieved, usually the stress at the time of stick slip or creep. At higher

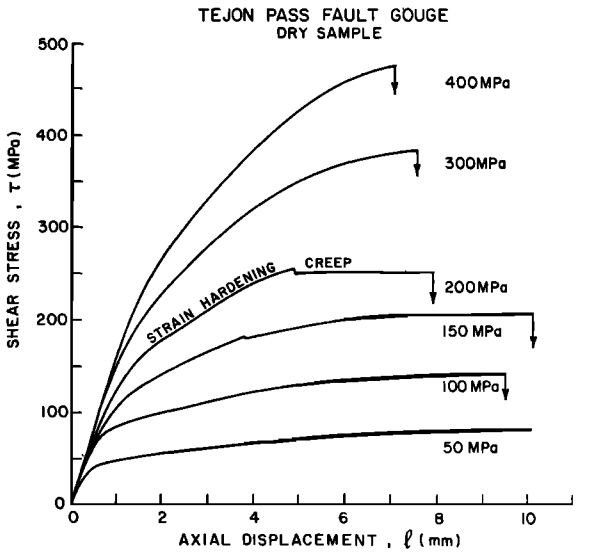

Fig. 5. Shear stress as a function of axial displacement for dry Tejon Pass gouge under confining pressures from 50 to 400 MPa, showing strain hardening and premonitory creep stages. Stick slip failure is indicated by downward arrows.

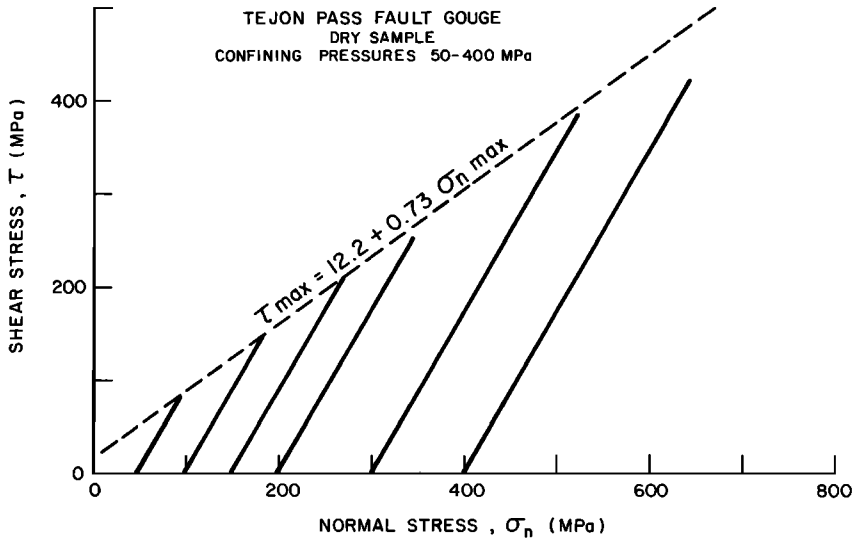

Fig. 6. Shear stress–normal stress relation for the strength curves of Figure 5. Confining pressures for each experiment correspond to the initial normal stress.

confining pressures (200, 300, and 400 MPa), the τ-σ_n lines fell short of this failure envelope because failure envelopes for rocks are not, in general, linear over a large range of pressures.

The strength properties of the wet Tejon gouge (Figure 7) were in many ways similar to the dry experiments. However, because of the saturated state of the samples, the yield strengths were lower. No creeping stage was observed during these experiments. Stable sliding continued with uniformly increasing stresses for the duration of the experiment with no major stick slip events, as seen in the dry experiments. Again, the amount of strain hardening increased with higher confining pressures. Strength and strain hardening are not expected to rise indefinitely at larger displacements, as Figure 7 would imply. The limitations of the experimental technique prevent us from observing the variation in stress-strain behavior after 10 mm of displacement or at much higher confining pressures. However, we can assume that the strength curves for dry samples will be the limiting case at each confining pressure. If so, then the strength increase of saturated samples may be expected to level off or exhibit stick slip behavior at larger strains than we have observed, probably at some shear stress lower than for the equivalent dry case.

One might argue that the strain-hardening effect observed in these saturated samples is caused by the dissipation of high pore pressure that could result from the initial hydrostatic loading of the sample or from the differential stress during shearing. The effective stress would then rise correspondingly with time (and hence displacement), resulting in an apparent strengthening of the gouge. This hypothesis was tested in a separate series of permeability experiments (to be reported elsewhere), using the same samples as our present study. Pore volume and flow rate measurements after hydrostatic loading and after various amounts of gouge shearing showed that (1) pore pressure equilibrium after initial loading was reached fairly quickly depending on the confining pressure due to the thinness of the gouge layer (sliding was not started until this stage was completed), and (2) after each episode of sliding, water was able to flow into the gouge layer at a constant rate with or without the differential shear

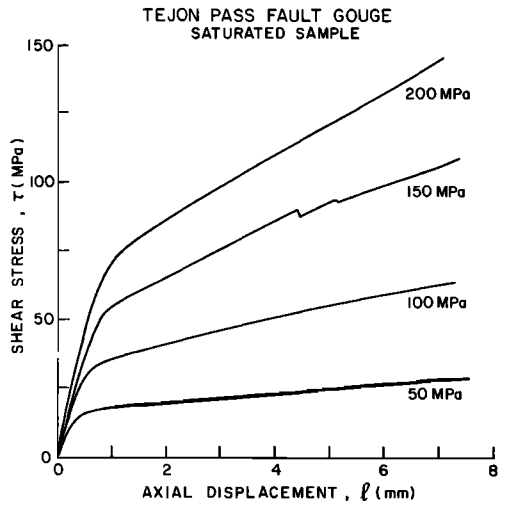

Fig. 7. Shear stress as a function of axial displacement for saturated Tejon Pass fault gouge. Confining pressures from 50 to 200 MPa are indicated next to the curves.

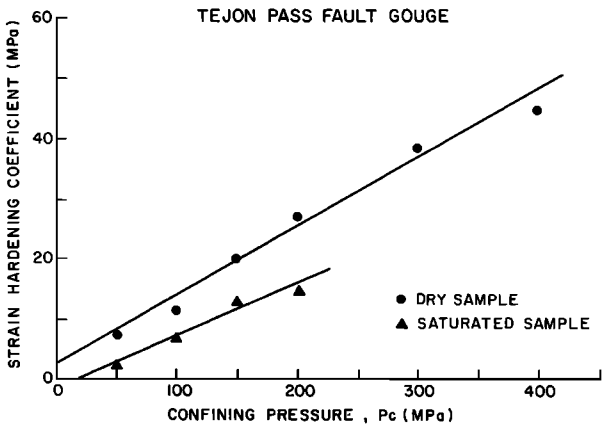

Fig. 8. Strain-hardening coefficients for dry and wet Tejon Pass fault gouge.

stress. Therefore, dewatering of the gouge was not the cause of strain hardening in the saturated samples.

To compare the amount of strengthening at each pressure, we define a 'strain-hardening coefficient' as the slope of the stress-strain curve during the strain-hardening period (not to be confused with the shear modulus G, which refers to the slope of the elastic portion of the stress-strain curve of a solid under applied shear stress). When this strain-hardening coefficient was plotted against confining pressure, a linear relationship was apparent for both the wet and dry cases (Figure 8), indicating that hardening is strongly controlled by pressure. It should be noted that during triaxial loading, normal stresses are rising, which causes an associated rise in shear stresses. Strain hardening may be more apparent in these triaxial experiments due to the angled saw cut than during biaxial loading, where normal stresses are constant. Biaxial experiments that appear to have no strain hardening may be masking an effect that would be apparent in a triaxial setup. Therefore hardening coefficient relationships such as those plotted in Figure 8 are not always comparable between these different experimental techniques.

Because the strain-hardening coefficients in Figure 8 are lower for the wet, drained samples than the dry samples, we might predict an even more pronounced effect when the gouges are not allowed to drain during deformation. This situation may be found either in natural formations of low permeability materials that are subjected to stress or in porous materials that are bounded by nearly impermeable rocks [*Berry*, 1973; *Bredehoeft and Hanshaw*, 1968]. Figure 9 shows a striking example of how the presence of water affects the strength, stability, and strain-hardening properties of the gouge. The undrained sample is the extreme case of low strength and stable sliding. As confining pressure was applied, the trapped pore fluids became overpressured, allowing slip to proceed easily with little rise in shear stress. The absence of excess pore pressure in the drained samples increased the strength by around 100 MPa, and the hardening coefficient became substantially larger. These features were even more pronounced in the dry experients where, in addition, sliding became unstable and ended in stick slip failure.

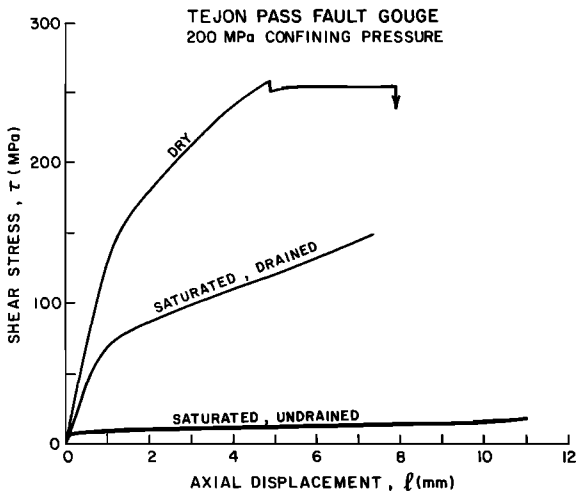

Fig. 9. Strength of Tejon Pass fault gouge as a function of water saturation. Stick slip failure of the dry sample is indicated by the downward arrow.

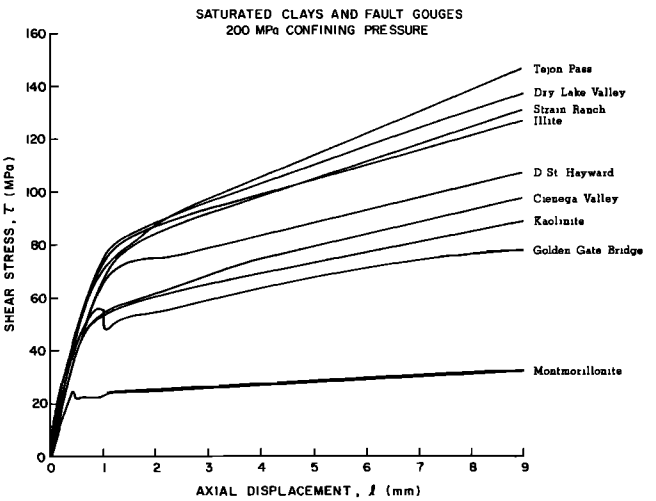

Fig. 10. Shear stress as a function of displacement for gouges of variable composition from the San Andreas and Hayward faults as well as three pure clay samples. All the gouges were deformed at 200-MPa confining pressure.

In the final series of the experiments, saturated gouges of variable composition were deformed at 200-MPa confining pressure (Figure 10). These strength curves are remarkably consistent with the observations of the Tejon Pass gouge; the slopes of the sliding curves are generally higher for each stronger gouge. The amount of strain hardening is apparently a function of the strength for these wet, drained samples, and it is not necessarily systematic with the composition. Compare, for instance, the relative strengths of the Tejon Pass and Cienega Valley samples. They have similar compositions of predominantly montmorillonite and mixed-layer clays and yet the strengths differ by up to nearly 50 MPa. Although the Tejon Pass sample was the strongest gouge of the group, it is composed largely of montmorillonite, which had an anomalously low strength. An even more striking comparison can be made between the Golden Gate Bridge and D Street Hayward samples. These two have nearly identical grain size and compositions (pure serpentine), but again the strengths are substantially different. At this time, the effect of composition on the frictional strength is somewhat unpredictable.

This set of experiments also demonstrates that grain size is not a major factor controlling strength for samples of differing composition. The montmorillonite-rich gouges were very fine grained (94–98% less than 63 μm in diameter), the chlorite-rich Strain Ranch gouge was intermediate (61% less than 63 μm), and the serpentine gouges were coarser (25% less than 63 μm). The strength curves do not fall in this sequence. Our main conclusion from Figure 10, amid these seemingly unsystematic relationships, is that the amount of strain hardening does increase with strength as was observed earlier, even for these samples of diverse character. Therefore, the strain hardening of granular specimens during shearing must be a material property.

The strength curves plotted in Figure 10 can be used to determine the coefficient of friction as a function of shear strain for these samples, as illustrated in the left-hand side of Figure 11. The origin of the strain axis has been shifted to the 'elbow' of the stress-strain curves, so as to distinguish the initial elastic compaction of the gouge from actual shear

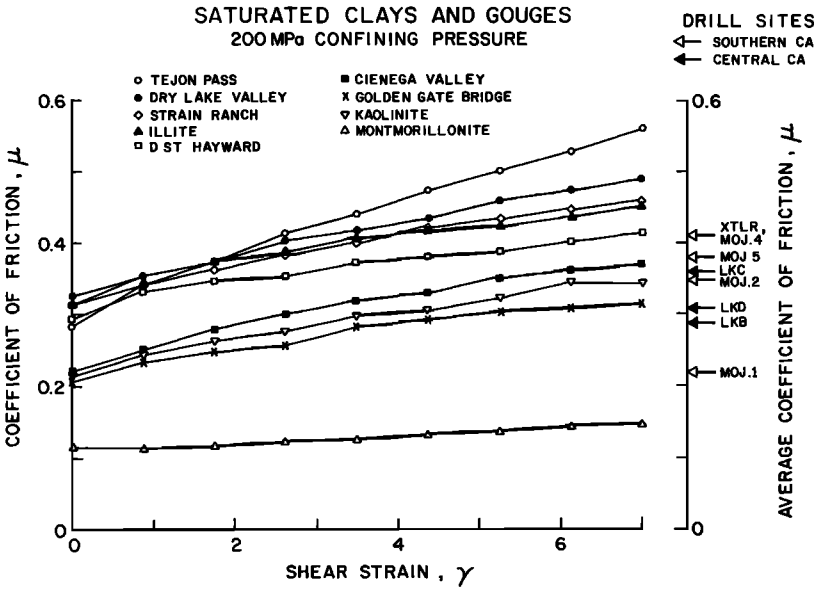

Fig. 11. The coefficient of friction as a function of shear strain for saturated gouges and pure clays under 200-MPa confining pressure. The strain axis begins at the 'elbow' of the associated strength in curves in Figure 10 to distinguish initial compaction from shear strain. For comparison of laboratory and field measurements, the far right of the figure shows friction data for southern and central California drill sites as determined by hydrofracturing techniques [*Zoback et al.*, 1980]. Arrows indicate the average coefficients of friction (±0.06) from stress measurements at several depths.

strain. Coefficients of friction ranged between 0.21 and 0.55 (with the exception of pure montmorillonite) and increased with strain in response to the strengthening of the material.

For comparison, the right side of the figure shows the average coefficient of friction around several boreholes near the San Andreas fault in central California and the Mojave desert, as measured by *Zoback et al.* [1980]. They determined the state of stress of hydrofracturing techniques to a depth of 850 m at locations between 2 and 34 km from the fault. From the principal stress measurements [*Zoback et al.*, 1980, p. 6159], the effective normal stress, shear stress, and hence coefficient of friction μ can be calculated at each depth. Because the stresses rise fairly uniformly within the depth interval sampled (with the exception of the shallowest hole, Moj. 1), μ does not vary by more than about 10% within each hole. Most of the average μ values fall within an interval between 0.29 and 0.41.

The coefficients of friction of our laboratory samples are remarkably consistent with the field measurements (although it is not clear what values of shear strain are most appropriate for comparison). These two sets of data have one location in common; the Cienega Valley gouge sample was taken from one of the central California drill holes. It is interesting to note that the coefficient of friction of the gouge sample at higher strains is the same as the creeping central California value of about 0.35.

From the comparison of the laboratory and field data in Figure 11, we assume that samples collected near the surface are representative of materials found deeper within the fault zone. However, the extent of clay gouges at depth is an unsettled point.

Because laboratory experiments performed at 200-MPa pressure correspond to a depth in the earth greater than typical in situ measurements, it would be of interest to know if there is a significant variation of μ with confining pressure or, equivalently, depth. Coefficient of friction values at several confining pressures, calculated from the strength curves of the Tejon Pass gouge (Figures 5 and 7) under wet and dry conditions, are plotted in Figure 12. There are a number of striking differences between these two groups of curves. The μ values for the wet samples are much lower (0.3 to 0.55 wet, 0.4 to 0.85 dry), and the curves do not level off as quickly with strain as their dry counterparts. The saturated samples are characterized by higher friction with increasing pressure, whereas the dry samples exhibit the reverse trend; that is, μ decreases with pressure. At first glance this result might seem peculiar, as it implies that for dry samples at low values of stress, the friction is anomalously high. The paradox is easily resolved if we take a look

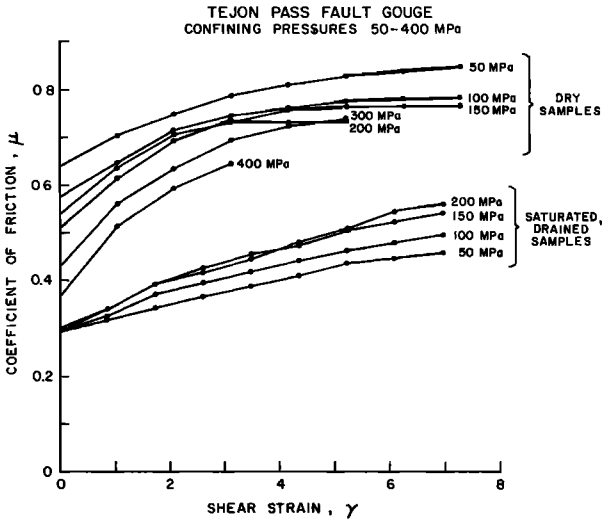

Fig. 12. Coefficient of friction as a function of shear strain for both dry and water-saturated Tejon Pass fault gouge at confining pressures from 50 to 400 MPa.

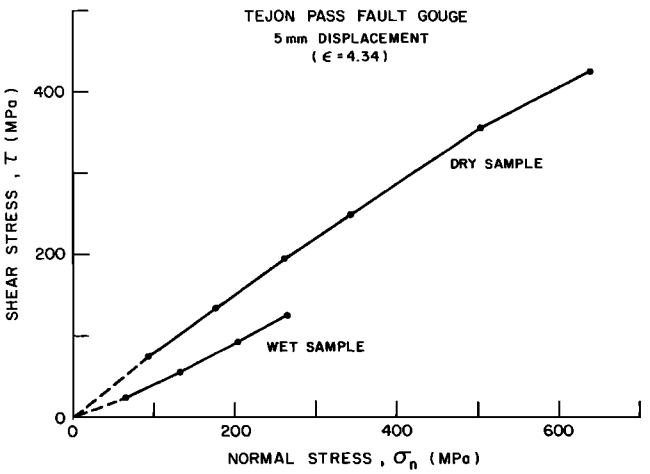

Fig. 13. Shear stress–normal stress data for saturated and dry Tejon Pass gouge at a strain of 4.34. The differing curvature of the wet and dry experiments explains the reverse trend of friction with confining pressure between the saturated and dry data of Figure 12.

at the actual τ-σ_n values from which these coefficients were calculated.

Figure 13 depicts the dry and wet τ-σ_n curves of the Tejon Pass gouge at 5/mm of displacement (ϵ = 4.34). This choice of strain is arbitrary; we could have used any other value of strain to illustrate the point. Although it would be convenient for analytical purposes to draw straight lines through the data whose slopes are the respective coefficients of friction, the true τ-σ_n relation is actually a curved function. In the dry case, the line is slightly concave downward, accentuated by the fact that we extent the line to the origin. Therefore, σ_n increases faster than τ along the curve, and as a result, the slope $d\tau/d\sigma_n$ must decrease with higher pressure, in accordance with the results of Figure 12. The wet curve, on the other hand, has a positive second derivative yielding an increase in $d\tau/d\sigma_n$ as σ_n increases. This results in a higher friction at greater pressures, just the opposite of the dry gouges. A straight-line approximation of these two curves would also lead to the observed reverse trend of friction with confining pressure between the dry and wet samples because of the opposite sign of the τ intercept in each case. The physical mechanism responsible for this behavior is not well understood at present.

Shear and normal stress values for a number of the dry fault gouges coincide well with the friction data collected by *Byerlee* [1978] for several different rock types. In that study as well as in this investigation, certain pure clays showed anomalously low friction. However, our highest friction gouges contain sizable amounts of these weaker constituents (montmorillonite in particular). Therefore, the friction of these samples is not necessarily controlled by the weakest member, possibly because slip plane fabrics of low-friction minerals are not extensively developed.

Discussion

The particular behavior of these fault gouges might best be understood in terms of the grain-to-grain mechanisms of deformation. *Engelder et al.* [1975] proposed that stable sliding of rock-gouge assemblages occurs when the rock is able to ride on a layer of cataclastically flowing gouge. Stick slip, on the other hand, results when the rock slips along the rock-gouge interface. The transition between these two sliding mechanisms occurs when it becomes sufficiently difficult for the grains to flow internally—in part a consequence of the compaction, grain cracking, and grain size reduction during cataclasis. As the grains become compacted and interlocked under pressure and conditions of decreasing pore volume, it becomes more difficult for particles to slide over one another. Instead, one grain breaks through the asperities of the next, rounding the edges of angular particles and increasing the surface area of the gouge, as demonstrated by *Jones* [1981]. As a result of this greater internal contact area and the additional energy required to crack rather than override grains, a larger shear force is necessary to overcome friction. This rather simplified view of gouge deformation is consistent with the gouge strengthening observed at higher confining pressures and strain. These factors will tend to enhance the compaction and interlocking of grains, thereby creating a greater frictional resistance to shear.

Eventually, for the dry gouges of this study, this frictional resistance decreased into a period of stable sliding prior to stick slip failure, so-called premonitory creep. This has been widely observed with other rock types, although the physical mechanism is not well understood [*Logan*, 1977; *Scholz et al.*, 1972; *Engelder et al.*, 1975]. *Byerlee and Summers* [1975] observed from testing granite specimens that the amount of stable sliding prior to slip decreased at higher pressures until stick slip occurred with almost no creep. This is also true of our natural fault gouges. These observations support the notion that near-surface fault creep may be the preferred deformation mechanism in the shallow crust where lithostatic stresses are low, whereas deeper in the earth, brittle failure is expected to predominate [*Scholz et al.*, 1972; *Byerlee and Summers*, 1975].

Surface premonitory creep events have been reported in a number of places, the most notable at the Cienega Winery near Hollister, California (*Nason*, 1973]. There the slip rate increased along the San Andreas fault from the norm of 12 to 20 mm/yr for 2 years prior to the earthquakes of April 1961. After the earthquakes, no creep occurred for 18 months. Following this quiescent period, creep gradually resumed at the lower rate of 12 mm/yr.

Are both this steady creep, observed at the winery, and the relatively low strength of our Cienega Valley gouge measured in the laboratory an indication that fault gouges are inherently weaker in the creeping central California area than in the 'locked' regions to the north and south? This hypothesis has been called upon in the past to explain the regional characteristics of movement along the San Andreas fault. Presumably, the 'locked' regions have different material properties that can support higher stresses until stress is suddenly released as earthquakes rather than through steady state creep. Although this strength-location correlation is borne out by certain of the samples in this study (e.g., Tejon Pass and Strain Ranch gouges are relatively strong and are located in 'locked' regions), there are an equal number of counterexamples among the limited set of specimens tested here (compare Figures 1 and 10). For instance, the Dry Lake Valley gouge, collected from a presently active region of the fault, is nearly as strong as the Tejon Pass sample. We might expect it to behave more like the Cienega Valley gouge, which is located nearby and has a similar mineralogical composition. Assuming that our laboratory samples are representative of the gouge material at depth, the inconsis-

tencies in strength and regional slip patterns indicate that there are other factors to be considered besides fundamental material differences, such as stress state and hydrologic characteristics. Therefore, it would be unwise to generalize about gouge strength by regional earthquake behavior alone. There was no intrinsically weak central California-type gouge indicated by our studies.

These inconsistencies might be reconciled in light of the stabilizing influence of pore water, particularly at greater than hydrostatic pressures [*Wang and Mao*, 1979; *Irwin and Barnes*, 1975; *O'Neil and Hanks*, 1980; *Stesky and Brace*, 1973]. *Berry* [1973] concluded from a series of field measurements that high fluid potentials are present in Franciscan rocks to the east of the San Andreas fault. *Raleigh and Evernden* [1981] suggest that low seismic velocities coincident with the San Andreas fault trace also indicated that fluid pressures must be high in this zone. Such a condition requires an extremely low permeability fault material in order to maintain the anomalous pore pressure. *Morrow et al.* [1981] and *Chu et al.* [1981] found permeabilities of a few nanodarcies to several tens of nanodarcies for fault gouges under typical crustal conditions, thus confirming that such fluid pressures are possible. Are anomalous pore pressures maintained over long periods of time in these low permeability gouges? This is a difficult question to answer, and one that argues against the high pore pressure, low shear strength notion of faults. However, M. D. Zoback (personal communication, 1980) found high-pressure gas trapped within clays in the San Andreas fault at fairly shallow depth, proving that high pore pressures can be maintained in this low-permeability material, at least over some length of time.

On the other hand, the strength and coefficients of friction that we have measured during low pressure (drained) experiments are consistent with the coefficient of friction determined from in situ stress measurements in central California and the Mojave desert [*Zoback et al.*, 1980]. These findings would argue that stresses are higher on the fault than the excess pore pressure model discussed above would predict and higher than the low shear stresses (~100 bars) advocated by *Brune et al.* [1969] based on the absence of a heat flow anomaly over the San Andreas fault. *Scholz et al.* [1979] suggest that the low heat flow anomaly can be accounted for while still maintaining high shear stresses on the fault if massive water circulation dissipates the heat away. If this is the case, then we must be able to explain this water circulation in light of the low-permeability materials identified in fault zones. Numerous smaller faults exist around the San Andreas, which may also contain clay-rich gouges that could act as partial barriers to this circulation.

SUMMARY OF RESULTS

1. These experiments have demonstrated that neither the frictional tractions that resist lateral motion at the ends of the sample nor the strength of the jacket material had an effect on the strain-hardening properties of the fault gouge during shear. Therefore, the observed strain hardening is a material property of the gouge not an artifact of the experimental setup.

2. Strain hardening increased systematically as confining pressure increased for both wet and dry gouges.

3. Strain hardening of the dry gouge occurred for progressively smaller amounts of displacement before the onset of creep at each higher confining pressure. This creeping stage was terminated by sudden stick-slip in all of the dry experiments except that at 50-MPa confining pressure. No creep or large stress drops were observed for the saturated gouge.

4. The presence of water lowered strength, friction, and amount of strain hardening of the samples.

5. The strength of the different gouges did not correlate well with the mineral composition, grain size distribution, or location of the sample in relation to the creeping or 'locked' sections of the San Andreas fault.

6. The coefficient of friction for the various fault gouges and pure clays ranged from around 0.21 to 0.55 under saturated, drained conditions at 200-MPa confining pressure with the exception of the anomalously weak pure montmorillonite sample. These values of friction are comparable to those determined from in situ stress measurements along the San Andreas fault in central and southern California.

REFERENCES

Berry, F. A., High fluid potentials in California coast ranges and their tectonic significance, *Am. Assoc. Pet. Geol. Bull.*, *57*, 1219, 1973.

Bredehoeft, J. D., and B. B. Hanshaw. On the maintenance of anomalous fluid pressures, I, Thick sedimentary sequences, *Geol. Soc. Am. Bull.*, *79*, 1097, 1968.

Brune, J. N., T. L. Henyey, and R. F. Roy, Heat flow, stress, and rate of slip along the San Andreas fault, California, *J. Geophys. Res.*, *74*, 3821, 1969.

Byerlee, J. D., Brittle-ductile transition in rocks, *J. Geophys. Res.*, *73*, 4741, 1968.

Byerlee, J. D., Friction of rocks, *Pure Appl. Geophys.*, *116*, 615, 1978.

Byerlee, J. D., and R. Summers, Stable sliding preceding stick-slip on fault surfaces in granite at high pressure, *Pure Appl. Geophys.*, *113*, 63, 1975.

Chu, C. L., C. Y. Wang, and W. Lin, Permeability and frictional properties of San Andreas fault gouges, *Geophys. Res. Lett.*, *8*, 565, 1981.

Engelder, J. T., J. M. Logan, and J. Handin, The sliding characteristics of sandstone on quartz fault-gouge, *Pure Appl. Geophys.*, *113*, 69, 1975.

Irwin, W. P., and I. Barnes, Effect of geologic structure and metamorphic fluids on seismic behavior of the San Andreas fault system in central and northern California, *Geology*, *3*, 713, 1975.

Jones, L. M., Field and laboratory studies of the mechanics of faulting, Ph.D. thesis, Mass. Inst. of Technol. Cambridge, 1981.

Lambe, T. W., and R. V. Whitman, *Soil Mechanics*, John Wiley, New York, 1969.

Logan, J. M., Crep, stable sliding and premonitory slip, in *Proceedings of Conference II: Experimental Studies of Rock Friction With Application to Earthquake Prediction*, edited by J. F. Evernden, p. 205, U.S. Geological Survey, Menlo Park, Calif., 1977.

Mitchell, J. K., *Fundamentals of Soil Behavior*, John Wiley, New York, 1976.

Morrow, C. A., L. Q. Shi, and J. D. Byerlee, Permeability and strength of San Andreas fault gouge under high pressure, *Geophys. Res. Lett.*, *8*, 325, 1981.

Nason, R. D., Fault creep and earthquakes on the San Andras fault, Proceedings of the Conference on Tectonic Problems of the San Andreas Fault System: Stanford, Calif., *Stanford Univ. Publ. Geol. Sci.*, *13*, 275, 1973.

O'Neil, J. R., and T. C. Hanks, Geochemical evidence for water-rock interaction along the San Andreas and Garlock faults of California, *J. Geophys. Res.*, *85*, 6286, 1980.

Raleigh, B., and J. Evernden, Case for low deviatoric stress in the lithosphere, in *Mechanical Behavior of Crustal Rocks*, *Geophys. Monogr. Ser.*, vol. 24, edited by N. L. Carter et al., p. 173, AGU, Washington, D.C., 1981.

Scholz, C. H., P. Molnar, and T. Johnson, Detailed studies of frictional sliding of granite and implications for the earthquake mechanism, *J. Geophys. Res.*, *77*, 6392, 1972.

Scholz, C. H., J. Beavan, and T. C. Hanks, Frictional metamor-

phism, argon depletion, and tectonic stress on the Alpine fault, New Zealand, *J. Geophys. Res.*, *84*, 6700, 1979.
Shimamoto, T., and J. M. Logan, Effects of simulated fault gouge on the sliding behavior of Tennessee sandstone: Nonclay gouges, *J. Geophys. Res.*, *86*, 2902, 1981.
Stesky, R. M., Rock friction-effect of confining pressure, temperature and pore presure, *Pure Appl. Geophys.*, *116*, 690, 1978.
Stesky, R. M., and W. F. Brace, Estimation of frictional stress on the San Andreas fault from laboratory measurements, Proceedings of the Conference on Tectonic Problems of the San Andreas Fault System: Stanford, Calif., *Stanford Univ. Publ. Geol. Sci.*, *13*, 206, 1973.
Summers, R., and J. D. Byerlee, A note on the effect of fault gouge composition on the stability of frictional sliding, *Int. J. Rock Mech. Min. Sci. Geomech. Abstr.*, *14*, 155, 1977*a*.
Summers, R., and J. D. Byerlee, Summary of results of frictional sliding studies, at confining pressures up to 6.98 kb, in selected rock materials, *U.S. Geol. Surv. Open File Rep.*, *77-142*, 1977*b*.
Wang, C., and N. H. Mao, Shearing of saturated clays in rock joints at high confining pressures, *Geophys. Res. Lett.*, *6*, 825, 1979.
Wang, C. Y., N. H. Mao and F. T. Wu, Mechanical properties of clays at high pressure, *J. Geophys. Res.*, *85*, 1462, 1980.
Zoback, M. D., and J. D. Byerlee, A note on the deformational behavior and permeability of crushed granite, *Int. J. Rock Mech. Min. Sci. Geomech. Abstr.*, *13*, 291, 1976.
Zoback, M. D., H. Tsukahara, and S. Hickman, Stress measurements at depth in the vicinity of the San Andreas fault: Implications for the magnitude of shear stress at depth, *J. Geophys. Res.*, *85*, 6157, 1980.

(Received December 21, 1981;
revised May 17, 1982;
accepted May 21, 1982.)